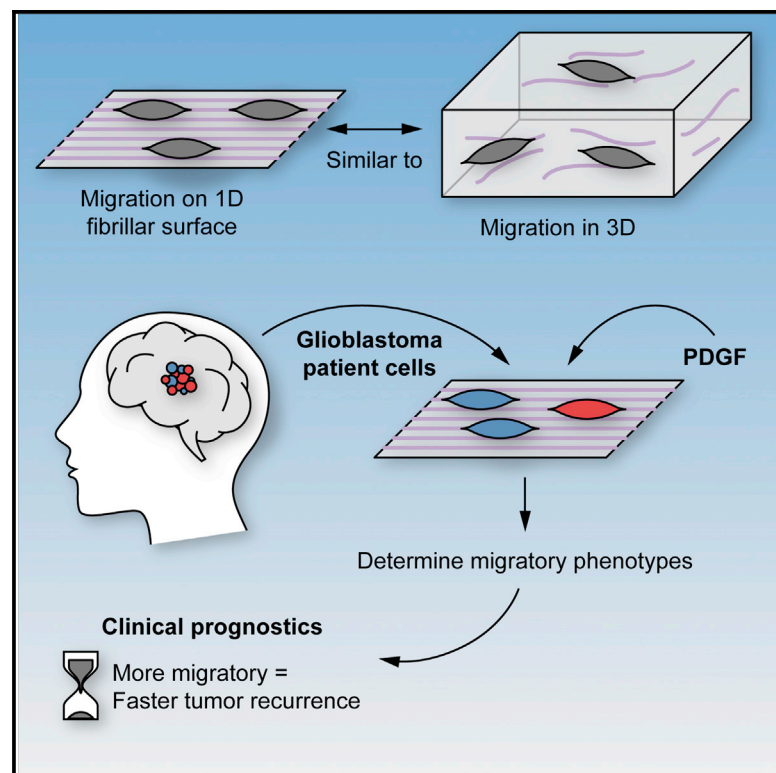


Cell Reports

Migration Phenotype of Brain-Cancer Cells Predicts Patient Outcomes

Graphical Abstract



Authors

Chris L. Smith, Onur Kilic, Paula Schiapparelli, ..., JinSeok Park, Alfredo Quiñones-Hinojosa, Andre Levchenko

Correspondence

aquinon2@jhmi.edu (A.Q.-H.), andre.levchenko@yale.edu (A.L.)

In Brief

Smith et al. describe a method to quantitatively screen cell migration responses of glioma cells to the growth factor PDGF. They demonstrate that this technique can differentiate glioma cells into two groups—strong and weak responders—which in turn strongly correlate with patient relapse and tumor location.

Highlights

- High-throughput analysis for tumor single-cell migration
- More sensitive and physiologically relevant than classical screening assays
- Glioma cells showing inter- and intra-patient differential sensitivity to PDGF
- Glioma cell sensitivity to PDGF correlating with tumor recurrence and tumor location



Migration Phenotype of Brain-Cancer Cells Predicts Patient Outcomes

Chris L. Smith,^{1,2} Onur Kilic,¹ Paula Schiapparelli,² Hugo Guerrero-Cazares,² Deok-Ho Kim,⁵ Neda I. Sedora-Roman,⁶ Saksham Gupta,^{2,3} Thomas O'Donnell,^{2,3} Kaisorn L. Chaichana,² Fausto J. Rodriguez,⁴ Sara Abbadi,² JinSeok Park,⁷ Alfredo Quiñones-Hinojosa,^{2,*} and Andre Levchenko^{7,*}

¹Department of Biomedical Engineering

²Department of Neurosurgery

³Department of Neuroscience

⁴Department of Pathology

Johns Hopkins University School of Medicine, Baltimore, MD 21231, USA

⁵Department of Bioengineering, University of Washington, Seattle, WA 98195, USA

⁶Department of Radiology, Beth Israel Deaconess Medical Center, Boston, MA 02215, USA

⁷Department of Biomedical Engineering and Yale Systems Biology Institute, Yale University, New Haven, CT 06516, USA

*Correspondence: aquinon2@jhmi.edu (A.Q.-H.), andre.levchenko@yale.edu (A.L.)

<http://dx.doi.org/10.1016/j.celrep.2016.05.042>

SUMMARY

Glioblastoma multiforme is a heterogeneous and infiltrative cancer with dismal prognosis. Studying the migratory behavior of tumor-derived cell populations can be informative, but it places a high premium on the precision of *in vitro* methods and the relevance of *in vivo* conditions. In particular, the analysis of 2D cell migration may not reflect invasion into 3D extracellular matrices *in vivo*. Here, we describe a method that allows time-resolved studies of primary cell migration with single-cell resolution on a fibrillar surface that closely mimics *in vivo* 3D migration. We used this platform to screen 14 patient-derived glioblastoma samples. We observed that the migratory phenotype of a subset of cells in response to platelet-derived growth factor was highly predictive of tumor location and recurrence in the clinic. Therefore, migratory phenotypic classifiers analyzed at the single-cell level in a patient-specific way can provide high diagnostic and prognostic value for invasive cancers.

INTRODUCTION

Aggressive cancers, such as glioblastoma multiforme (GBM), are of particular interest due to the heterogeneous nature of individual tumors (Snuderl et al., 2011; Szerlip et al., 2012) and high recurrence following surgical resection (Filippini et al., 2008; McGirt et al., 2009; Chaichana et al., 2013, 2014). Genomic and proteomic profiling can provide a wealth of information about tumor samples, including cancer-specific mutations and clinically relevant subclasses (Verhaak et al., 2010). However, these cell population-based analyses ignore the diversity of individual cells that can predetermine the aggressiveness of a given tumor. High-throughput genomic and proteomic single-cell ana-

lyses of multiple samples are not within reach of clinical applications (Kalisky et al., 2011; Meier et al., 2013). Furthermore, aggressive cell migration can be a product of multiple and distinct combinations of genetic alterations and would benefit from a complementary analysis of phenotypic properties at the individual cell level. As with many other cancers, individual GBM cells can spread from the primary tumor bulk, avoid detection, and form secondary tumor foci (Sahai, 2007). Growth factors, e.g., platelet-derived growth factor (PDGF), have emerged as enhancers of malignant potential in GBM, because they affect cell migration and proliferation (Fomchenko and Holland, 2007; Shih and Holland, 2006). Various components of the extracellular matrix (ECM), such as laminin, have also been implicated in modulation of cell migration (Friedl and Wolf, 2010; Petrie et al., 2009; Wirtz et al., 2011; Anton et al., 1999; Porcionatto, 2006). Directional cell migration can be guided by a variety of mechanical cues presented by ECM structures ranging in size from nanometers to microns (Kim et al., 2009a, 2012; Park et al., 2016). Therefore, a challenge is to develop an experimental platform that will model the mechano-chemical cellular milieu yet remain simple and accessible to allow practical, high-throughput use. In this study, we demonstrate that single-cell-resolution phenotypic screening holds great promise in prognostic analysis of glioblastoma samples. We found that the clinical outcome of GBM tumors strongly correlated with the response to two environmental inputs: the nanotopography and the growth factor PDGF. The ability to observe this responsiveness at the single-cell level and thus examine different cell subpopulations was critical for the success of this phenotypic analysis, revealing correlations with such critical prognostic tumor characteristics as time of recurrence after resection.

RESULTS

Construction and Application of a Phenotypic-Screening Platform

To create 1D fibrillar surfaces that mimic nanometer-scale features of the 3D ECM microenvironment, we fabricated

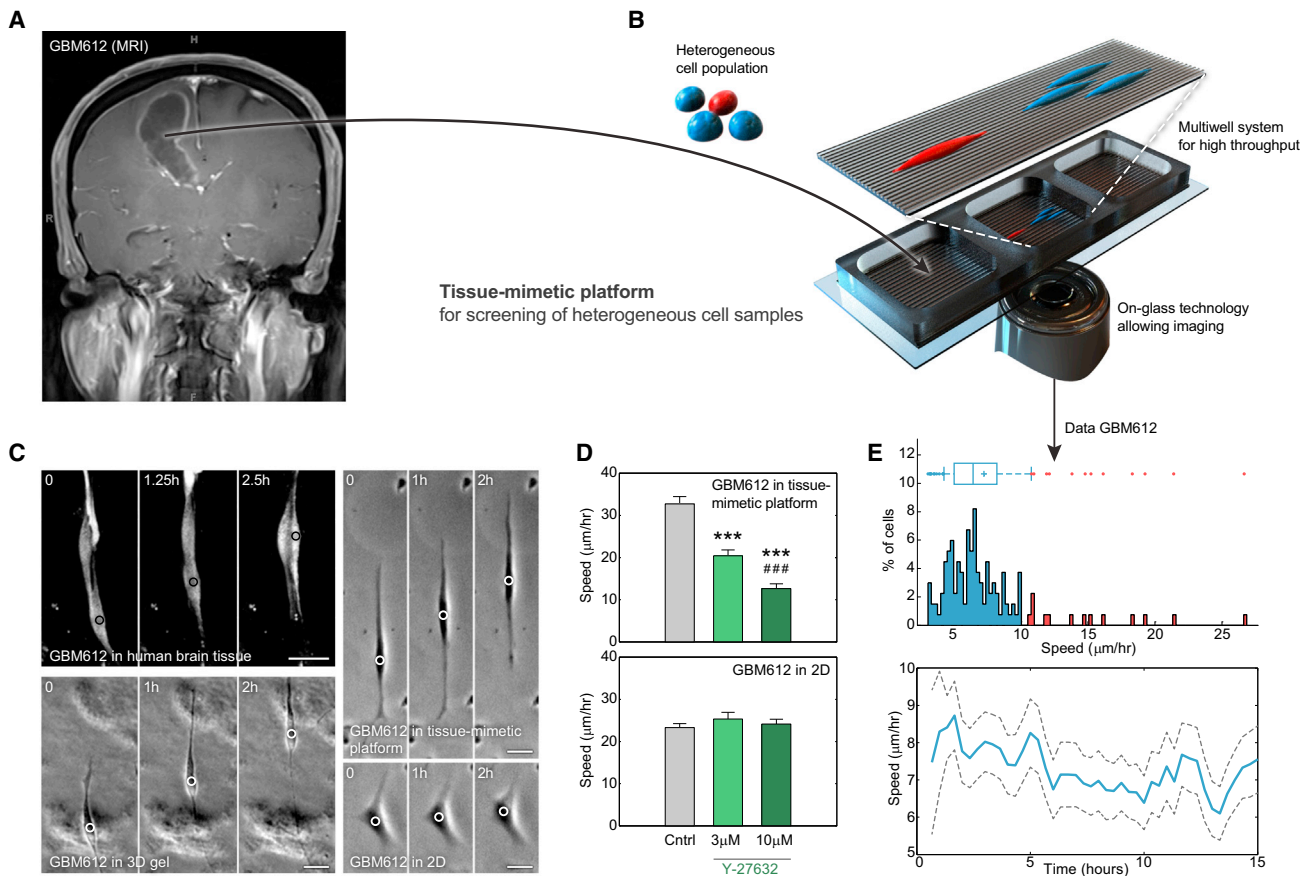


Figure 1. Phenotypic Screening of Heterogeneous Cell Populations Recapitulates the Microenvironment of Migrating Cells

(A) Cells with heterogeneous phenotypes are isolated from a patient's tumor (MRI of tumor for sample GBM 612).

(B) The cells are seeded on a platform that has a multi-well structure, allowing testing of multiple conditions, and is an on-glass technology, allowing direct imaging of migration and morphology with single-cell resolution.

(C) Images show that GBM 612 cells migrating on the platform have similar morphology and migration speed compared to GBM 612 cells migrating in ex vivo human brain tissue and 3D Matrigel. In comparison, cells migrating on flat surfaces are not polarized and have reduced migration speeds compared to the other cases (see [Supplemental Information](#)) (scale bars, 25 μm ; duration between each frame, 1 hr).

(D) ROCK inhibitor (Y-27632) affects migration of GBM 612 cells on tissue-mimetic substrates and flat surfaces ($n = 30$ cells, mean + SEM, *** $p < 0.0001$, *paired against control group, #paired against 3 μM group, Kruskal-Wallis one-way ANOVA on ranks, Dunn's method).

(E) The platform provides important information on the migration response of heterogeneous cell populations. GBM 612 samples show a subpopulation of cells whose migration is fast and stable over time.

topographic patterns consisting of regular, parallel ridges (Figures 1A, 1B, and S1A–S1C) similar in size to those found in the brain tissue ECM (Kim et al., 2009b; Bellail et al., 2004; Ottani et al., 2001). We explored how well cell migration on the quasi-3D, fibrillar topography approximated cell migration in a true 3D ECM environment. We compared the morphology, directionality, and speed of GBM 612 cells on our platform and cells migrating in distinct 3D settings: Matrigel matrix and organotypic human brain slice cultures (Figure 1C). We found that cell morphology on fibrillar, but not flat, surfaces mirrored the characteristic cell shapes found in 3D environments. Cell morphology in collagen 3D matrices was similar to that observed in our tissue mimetic platform (Huang et al., 2016). Furthermore, in contrast to 2D surfaces, migration speed was enhanced to levels similar to those observed in 3D settings (Figure 1C), displaying essentially 1D migration patterns. We replicated the same observations us-

ing other patient-derived cell lines (GBM 318 and GBM 276) (Figures S1B, S1D, and S1J). Consistent with a tendency of mobile cells to align parallel to oriented topographic structures (Friedl and Wolf, 2010), the direction of cell migration was strongly biased along the axis of the ridge pattern (Figures S1D and S1J; Movies S1, S2, and S3). Compared to smooth surfaces, cells cultured on the platform showed increased cell area and spindle shape factor (Figures S1E, S1H, and S1I), and their migration was enhanced based on the three metrics scored: average speed, alignment, and persistence (Figures S1F, S1G, S1K, and S1L). These results suggested a high degree of similarity between our platform and the true 3D microenvironments, possibly due to similar molecular mechanisms observed in cells migrating on 1D fibrillar surfaces and 3D matrices but distinct from those observed in cells cultured on 2D surfaces (Doyle et al., 2009). To test the similarity between 1D fibrillar surfaces

and 3D microenvironments, we analyzed the effect of the Rho-associated protein kinase (ROCK) inhibitor Y-27632 on the migration of GBM 612 cells (Figure 1D). We found that Y-27632 inhibited migration on fibrillar surfaces but not on flat surfaces, suggesting that myosin II plays a role in migration on the fibrillar surfaces, similar to findings in vivo (Beadle et al., 2008). We replicated these experiments with GBM 965 (Figures S1M and S1N). Using the multi-well setup of the device, we then explored the influence of two critical environmental cues: ECM density and growth factor (Figure S2). On the fibrillar surfaces, but not on the flat surfaces, we observed a strong dependence of cell velocity values on the surface density of laminin (Figures S2A, S2B, S2E, and S2F). The density at which cell migration speed was maximized was used in all subsequent experiments. Next, we examined the distributions of cell velocities. We found that cell migration was highly heterogeneous, displaying a substantial number of outliers, some exceeding the average cell migration 3- to 4-fold (Figure 1E). Our results confirm that the heterogeneity of cell behavior can be assessed in this platform, enabling the identification and characterization of rare cells with extreme properties.

Migratory Behavior of GBM Cells Can Be Altered in Response to a Combination of PDGF and Nanotopographic Cues

We explored whether 3D-like cell migration might be differentially sensitive to the effects of growth factors implicated in the onset and progression of glioma, e.g., PDGF-AA (PDGF). PDGF can control glioma cell proliferation, but its effect on GBM migration and invasion is less clear (Feng et al., 2012; Laurent et al., 2003). We tested the effects of PDGF on cell speed and persistence at different doses. On our platform, we found a dose-dependent response, with maximal motility achieved at intermediate PDGF concentrations (Figure S2D, S2G, and S2H). Similar experiments on flat substrata showed more limited response to PDGF (Figure S2C). We then explored whether the effect of PDGF could be ascribed to the activation of PDGF receptor alpha (PDGFR α). PDGFR α is thought to be the exclusive receptor for the PDGF-AA isoform employed in this study (Fomchenko and Holland, 2007). First, we examined the expression levels of PDGFR α in patient-derived cell lines by RT-PCR and immunoblotting (Figure 2A, 2B, and S3A–S3C). Then, we analyzed the migratory behavior of cells with low and high PDGFR α expression levels (GBM 253 and GBM 276, respectively). Following exposure to PDGF, we found an increase in cell speed and directionality of GBM 276 cells (high PDGFR α expression) but no response in GBM 253 (low PDGFR α expression) (Figures 2C–2G). To further ascertain that PDGFR α was functionally involved, we used the tyrosine kinase inhibitor imatinib and found that migration was attenuated to similar levels in both cell lines (Figures 2C, 2D, S3D, and S3E). However, a detailed analysis of the GBM 276 subpopulations showed a highly heterogeneous single-cell response to PDGF. In particular, only the fastest 25% quartile of cells responded to PDGF, with the response abrogated by the inhibitor (Figures 2F and 2G). Furthermore, the response of the slowest 25% quartile of GBM 276 cells was analogous to that of the PDGF-unresponsive cell line GBM 253 (Figures 2E and 2F). These results suggest

that migration of only a subset of cells is responsive to PDGF stimulation and that this subset represents the fastest cell subpopulation.

PDGF Enhances Invasiveness of Patient-Derived Cells In Vivo

Using orthotopic human GBM tumor models in mice (Figures S3F–S3J) (Garzon-Muvdi et al., 2012; Gonzalez-Perez et al., 2010), we explored the role of PDGF in tumor growth and survival. First, we examined the behavior of the xenografts using GBM 276 cells, cultured in the presence or absence of PDGF for 3 weeks before injection. This PDGF preculture selects for PDGF-responsive cells by stimulating their growth and enriching this cell subpopulation. In vitro analysis of GBM 276 cells showed that increased proliferation correlated with the PDGF-induced migratory response (Figures S3M–S3R). We observed significantly reduced survival of mice injected with PDGF-preconditioned cells ($n = 4$ each group) (Figure 2H). Although this result suggested the importance of highly PDGF-responsive cells for tumor aggressiveness, we could exclude other effects of prolonged PDGF exposure, e.g., transdifferentiation (Figure S3Q). We thus tested the putative role of PDGF in tumor spreading by supplying this factor exogenously in vivo to existing tumor xenografts via infusion pump (Figure S3F). Quantification of tumor size and qualitative analysis by a blinded neuropathologist suggested that continuous exposure of tumor xenografts to PDGF generated larger, more invasive tumors with more eccentric shapes (Figure S3K). These samples displayed features indicative of migration along fiber tracts. We also observed increased dispersion of GBM cells beyond the tumor margins (Figure S3L). These findings confirm the role of this growth factor in tumor induction and progression that was observed in other animal models (Fomchenko and Holland, 2007; Jackson et al., 2006; Lokker et al., 2002), and they are consistent with clinical data from The Cancer Genome Atlas (TCGA) (Goswami and Nakhshatri, 2013) suggesting significant correlation between PDGF expression and survival (Figure 2I). TCGA data did not show a similar correlation for PDGFR α expression (Figure 2J). Because the genomic data did not support the correlation between average PDGFR expression and patient outcomes, we examined the correlation between the tumor characteristics and the cell migration data obtained in the tissue-mimetic platform.

Screening Heterogeneity within and between Patient-Specific Tumor Samples

Heterogeneity of cell properties within the same tumor reflects subpopulations promoting tumor growth, progression, and therapeutic resistance (Snuderl et al., 2011). GBM is also known to have populations with distinct expression profiles of receptor tyrosine kinases, particularly PDGFR α (Snuderl et al., 2011; Szerlip et al., 2012). This heterogeneity requires analysis on the single-cell level, which is yielded in our platform with less than 1,000 cells (particularly beneficial for screening precious intraoperative human tissue specimens). We took advantage of the single-cell resolution to quantify the distribution of cell speed in control versus PDGF-exposed conditions and investigate the difference in migratory behaviors among 14 glioblastoma patients (Figures 3A–3C). We found both intra- and inter-patient

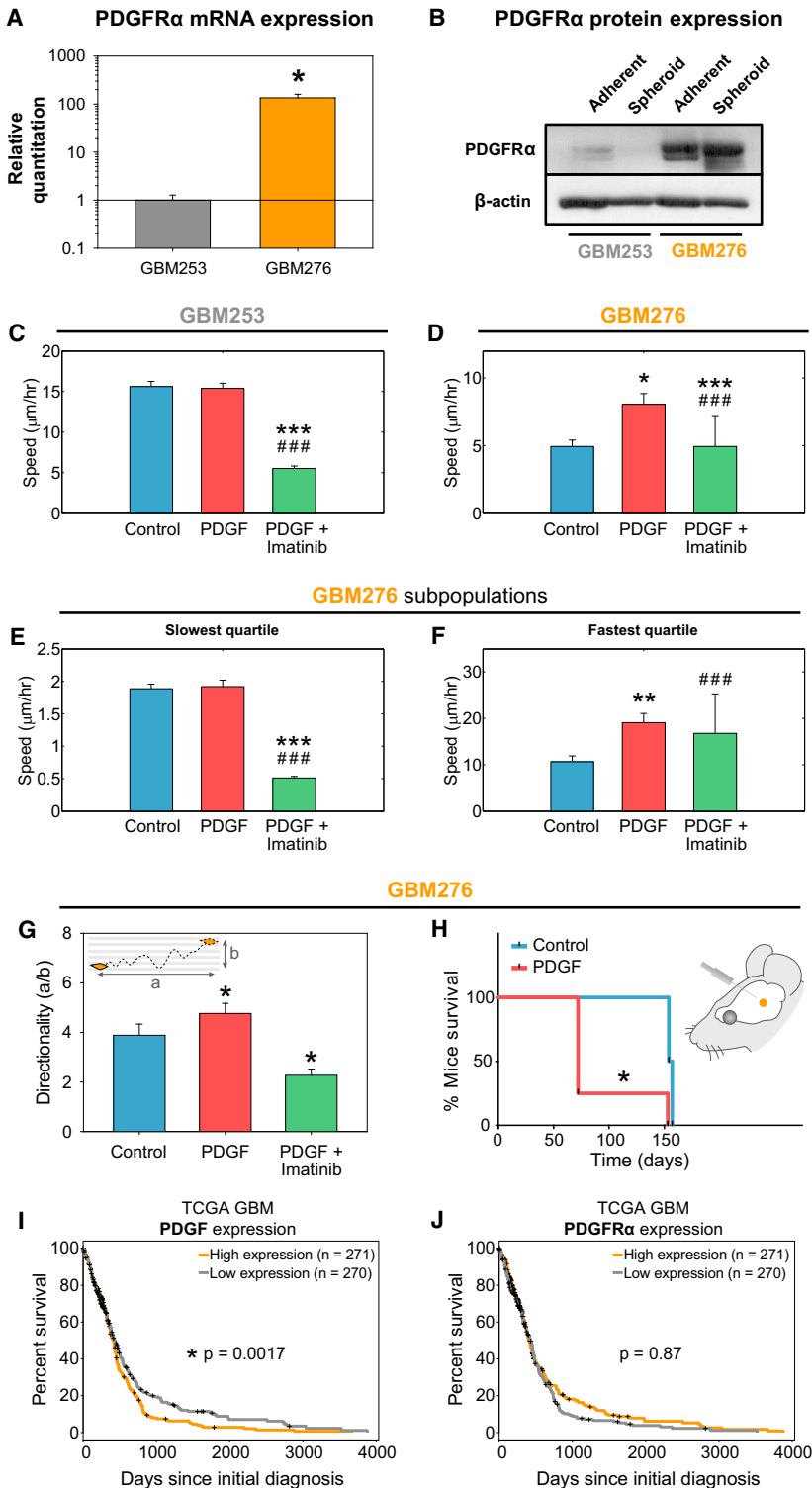


Figure 2. Migratory Response to PDGF Correlates with Tumor Characteristics Both In Vitro and In Vivo

(A) RT-PCR analysis of PDGFR α mRNA levels in responding sample GBM 276 and non-responding sample GBM 253 (n = 3, *p = 0.006, Student's t test). (B) Western blot for PDGFR α protein expression in GBM samples grown as adherent or spheroid cultures. (C and D) Quantification of migration speed of cell lines GBM 253 (C) and GBM 276 (D) in the presence of PDGF-AA (50 ng/ml) and imatinib (30 μ M) (n \approx 80 cells, mean + SEM, *p < 0.05, **p < 0.01, ***p < 0.001, *paired against control group, #paired against PDGF group, Kruskal-Wallis one-way ANOVA on ranks, Dunn's method) (asterisks indicate pairing against the control group, hash marks indicated pairing against the PDGF group). (E and F) Migration speed of GBM 276 for the slowest (E) and fastest (F) quartile of the cells (i.e., 25% of the slowest- and fastest-moving cells, respectively), showing that only a subpopulation responds to PDGF. (G) Quantification of migration measured by alignment of GBM 276 cells (*p < 0.05, Kruskal-Wallis one-way ANOVA on ranks, Dunn's method) (asterisks indicate comparisons to all other conditions). (H) Survival curves of mice injected with GBM 276 cells cultured in control spheroid conditions or in the presence of PDGF-AA (n = 4 mice per group, *p = 0.0097, Gehan-Breslow-Wilcoxon test). (I and J) Kaplan-Meier plots based on clinical TCGA data of GBM patients, comparing survival between high and low expression of PDGF-AA (I) and PDGFR α (J), respectively. The cohorts were divided at the median of the expression level of the respective gene.

ences (Figure 3A). Such masked responses and heterogeneities were also present in the time-domain data. For instance, two patient samples, GBM 501 and GBM 609, responded significantly to PDGF. However, for GBM 501, this response was not persistent throughout the experiment duration, in contrast to the response of GBM 609 (Figure 3B). Finally, the platform allowed us to investigate high-speed outliers. For example, for both the GBM 630 and the GBM 544 samples, cells experienced a significant increase in migration speed in response to PDGF. However, a detailed analysis of the speed distribution revealed that only for GBM 630 were fast-moving outliers clearly identifiable; GBM 544 showed a substantially more uniform response (Figure 3C).

We observed considerable differences in the cell speed across the spectrum of 14 patient-derived samples, both in the presence and in the absence of PDGF (Figure 3D).

differences in the cell population behavior. When analyzing GBM 499 cells based on their speed, the total population average showed no significant response to PDGF, while analysis of the 25% fastest quartile subpopulation revealed significant differ-

ences (Figure 3A). Such masked responses and heterogeneities were also present in the time-domain data. For instance, two patient samples, GBM 501 and GBM 609, responded significantly to PDGF. However, for GBM 501, this response was not persistent throughout the experiment duration, in contrast to the response of GBM 609 (Figure 3B). Finally, the platform allowed us to investigate high-speed outliers. For example, for both the GBM 630 and the GBM 544 samples, cells experienced a significant increase in migration speed in response to PDGF. However, a detailed analysis of the speed distribution revealed that only for GBM 630 were fast-moving outliers clearly identifiable; GBM 544 showed a substantially more uniform response (Figure 3C).

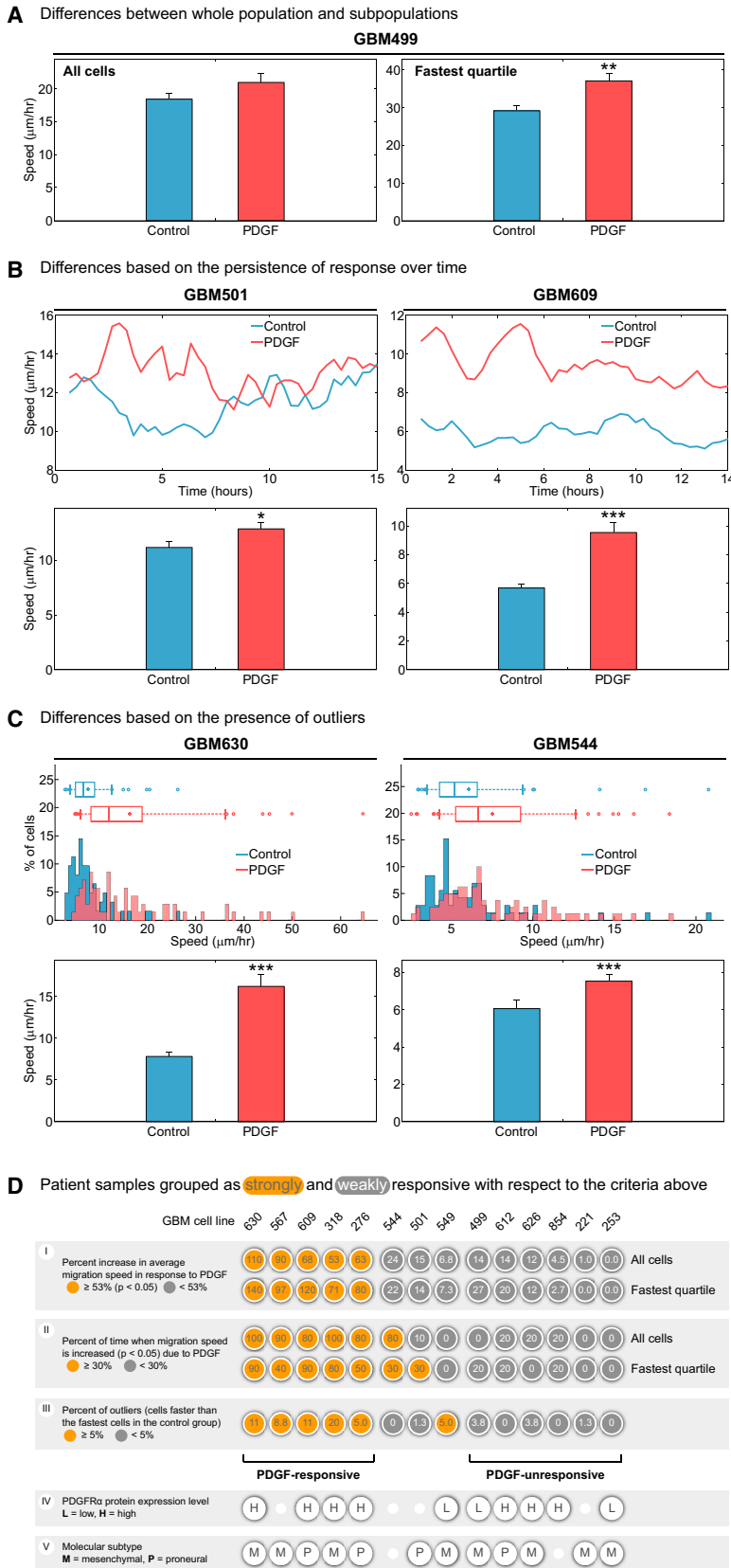


Figure 3. Information on Migration Speed Reveals Important Differences among Patient Samples in Response to PDGF

(A) Analyzing the fastest quartile (GBM 499) reveals that the subpopulations display a significant response to PDGF. In contrast, for the whole population, there is no significant response.

(B) Migration speed time lapse demonstrates that sample GBM 501 does not respond to PDGF at all times (compared to GBM 609); on average, however, both samples respond significantly to PDGF.

(C) Both GBM 630 and GBM 544 samples display a significant increase in average migration speed ($p < 0.05$, $**p < 0.01$, $***p < 0.001$, Wilcoxon rank-sum test). However, GBM 630 has a significantly larger number of fast outliers, while GBM 544 displays a uniform increase in speed.

(D) The platform allows patient sample classification based on multiple characteristics, permitting a better description of the heterogeneity of the samples. We compare 14 patients' GBM cell lines. The samples were grouped based on whether there is a significant increase ($p < 0.05$, Wilcoxon rank-sum test) in average migration speed in response to PDGF (group I) and whether this significant increase is persistent over time (group II). Furthermore, samples are grouped based on the number of outliers (cells faster than the fastest cells in the control group) with a threshold of 4 cells (5%, for a total of 80 cells) (group III). For reference, the PDGFR α protein expression level (group IV) and the subclass of the GBM cells (group V) are also provided.

(group II), and presence of outliers (group III) (Figure 3D). For each of these criteria, we identified PDGF-responsive and PDGF-unresponsive groups. There was overlap among strongly PDGF-responsive groups in all groups, which we thus treated as the consensus PDGF-responsive samples (marked in Figure 3D). However, several patient samples (GBM 544, GBM 549, and GBM 501) were PDGF responsive by some criteria. To determine whether PDGFR α expression level could serve as a molecular marker predictive of enhanced PDGF responsiveness, we assayed the tumor samples for expression of this receptor. Although all consensus PDGF-responsive samples had high expression of PDGFR α (Figures 2A, 2B, S3B, and S3C), similarly high levels of the receptor were found in several samples in the consensus PDGF-unresponsive group (GBM 626, GBM 612, and GBM 854). The failure of these samples to respond in migration experiments may be due to differences in downstream effectors of PDGFR α , stressing the difficulty of using molecular markers alone in the classification of the aggressive migration phenotype, as is evident from clinical data showing no correlation between PDGFR α expression and survival (Figure 2J). Differential expression of PDGFR α across the groups might also relate to the subtype of the patient tumors. A subclassification study of our GBM samples only yielded two subtypes: mesenchymal and proneural. Previous studies have observed higher amplification and mutation rates of the PDGFRA gene in the proneural subtype of GBM (Verhaak et al., 2010). We did not observe a clear correlation between expression of this gene and tumor subclass. High levels of PDGF-triggered cell migration can be achieved in various ways, and they may not be revealed by a simple molecular signature. However, the aggressive migration phenotype can be translated into enhanced invasiveness. These results highlight potential advantages of our single-cell phenotypic analysis.

Migratory Behavior Correlates with Clinical Tumor Characteristics

The degree of cell migration may reflect the propensity for invasive tumor spread. We examined more than 35 factors related to each patient's tumor, general health, and demographics (Table S1). We found that the migratory response of GBM samples to PDGF correlated with time to tumor recurrence after surgical resection (Figures 4A and 4B). This correlation was particularly significant when the analysis was focused on the consensus-responsive and consensus-unresponsive groups (Figure 4A). In comparisons to the whole-cell populations, correlations were more significant for the aggressively moving cells: either the fastest 25% of the cells or the outlier population (Figure 4B). We contrasted several characteristic tumor features visualized in the MRI of the patients with the responsiveness to PDGF (Figures 4C and 4D). Tumors from the consensus PDGF-responsive subset (Figure 4D) were larger and more spread out than those from the PDGF-unresponsive subset. We observed statistically significant differences in the anatomical location of the tumors; all consensus PDGF-responsive samples were in the frontal lobe (Figure 4E), but temporal lobe tumor samples commonly fell into the PDGF-unresponsive subgroup. Migration analysis of GBM cells revealed that higher directionality (i.e., alignment of the migration to the patterns) correlated with longer recurrence

times (univariate Cox analysis, $p = 0.002$) (Figures 4F and S4A). Because alignment of the migration is associated with the strength of cell-substrate adhesion (Kim et al., 2009a; Garzon-Muvdi et al., 2012), this result may reflect a higher propensity in more aligned cells to adhere to ECM, leading to retarded migratory response and delayed tumor spread. Blind, qualitative analysis of patient tumor samples by a neuropathologist revealed that the cells were small and that the tumors yielding PDGF-responsive samples had marked microvascular proliferation. The latter feature is commonly associated with advanced progression, receptor tyrosine kinase amplification, and worse prognosis (Louis, 2006; Fomchenko and Holland, 2007). PDGF-responsive samples emerged from tumors that resulted in shorter recurrence times, after controlling for factors known to be associated with recurrence (age, Karnofsky Performance Scale score, extent of resection, and adjuvant therapy) ($p = 0.0009$) (Table S1). However, survival times showed a less significant correlation to PDGF responsiveness with the limited number of patient samples tested (Figure S4B).

We supplemented these findings with comparisons to more traditional protein expression analyses. First, we segregated the tumor sample into groups based on PDGFR α expression, which revealed trends in patient tumor characteristics that were supportive of our migration analysis (Figure 3D). However, grouping the samples according to PDGFR α expression or molecular subclassification did not yield significant differences in predicting time to recurrence (Figures S4C and S4D). Moreover, the difference in tumor location between high- and low-expression groups was not statistically significant. Second, we mined the public Rembrandt database of glioblastoma patients to investigate the relationship between tumor location and PDGFR α expression. Examination of 47 patients revealed no significant relationship between the two characteristics (Figures S4E and S4F). Taken together, these findings suggest that RNA expression is a weaker predictor of patient outcomes than is our phenotypic migration analysis.

DISCUSSION

The heterogeneity and invasive nature of glioblastoma and other aggressive cancers highlights the importance of assaying cell migration as a phenotypic feature predictive of clinical outcomes. Here we describe a simple but information-rich experimental platform aimed at the analysis of primary patient samples on a single-cell level. This platform allows high-throughput screening of the effects of variable extracellular milieu. Using this method on a range of patient-derived samples and contrasting the results of the analysis with respective clinical information revealed substantial predictive power, particularly when cell migration was examined in conjunction with the effects of PDGF. This result strongly suggests that cell migration, as examined in structured, mechanically defined culture conditions, can be predictive of more complex in vivo invasion processes and can be a powerful phenotypic analysis tool with strong clinical implications. Prior attempts to examine glioma cell migration and its relationship to tumor progression (Friedlander et al., 1996) have used 2D surfaces and have not achieved such direct predictions of patient-specific tumor features as we have in the

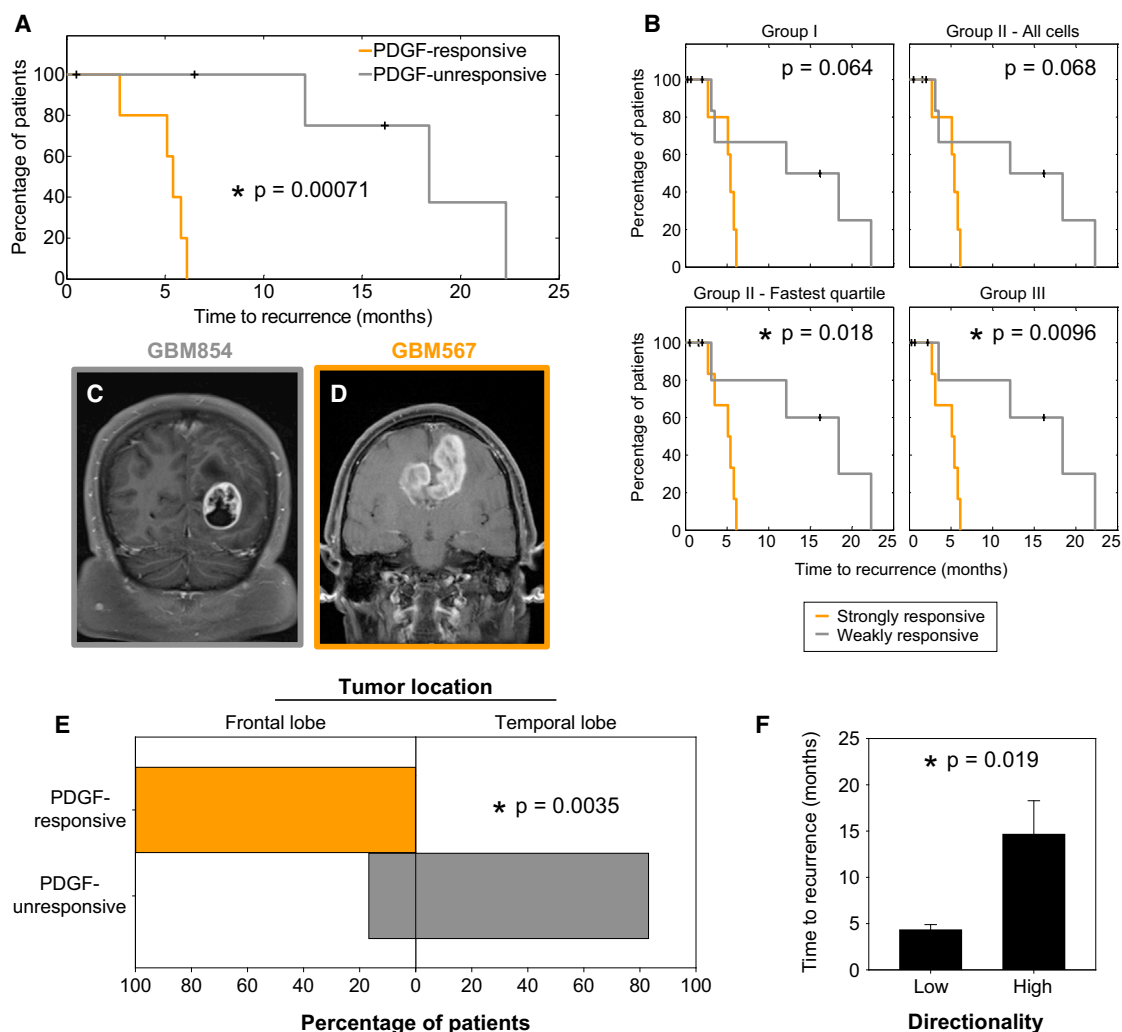


Figure 4. GBM Migratory Response to PDGF Correlates with Patient Tumor Characteristics

(A and B) Kaplan-Meier plots comparing recurrence between PDGF-responsive and PDGF-unresponsive groups ($n = 11$ patient tumors, consensus group) (A) and based on the criteria in Figure 3D ($n = 14$ patient tumors, weak and strong responders) (B). The p values were calculated using a two-tailed log-rank (Mantel-Cox) test.

(C and D) MRI scans of patients with tumors from the unresponsive group (C) and the responsive group (D).

(E) Distribution of PDGF-responsive and PDGF-unresponsive tumors that formed in specific locations in the brain ($n = 11$ patient tumors, Barnard's exact test).

(F) Time to recurrence for GBM samples separated into low-directionality (< 3.25) and high-directionality (≥ 3.25) groups ($n \geq 4$, mean + SEM, Wilcoxon rank-sum test) (the threshold of 3.25 was determined using linear discriminant analysis).

present work. This emphasizes the benefits of analyzing heterogeneities within samples and using surfaces that better mimic in vivo conditions.

The significant correlation of migratory behavior with time to recurrence and tumor location provides crucial insight into this disease. Recurrence of glioblastoma after tumor resection is the primary cause of death in patients and is one of the most important predictors of future patient outcomes (Chaichana et al., 2013, 2014). This study provides a simple method to glean information about these phenomena. Our finding that most PDGF-unresponsive tumors are derived from the temporal lobe could suggest that PDGF signaling is less critical to tumor progression in this region of the brain. Direct access to individual

cell migration analysis can be important for future treatment modalities. Our experimental platform has important advantages over 2D migration assays, because it provides a cellular environment similar to in vivo conditions (as evidenced in the similarity of several aspects of migration in ex vivo human brain tissue and a 3D hydrogel, e.g., increased cell polarity and migration speed). Previous studies have highlighted the importance of these factors in migration (Friedl and Wolf, 2010; Petrie et al., 2009; Kim et al., 2012; Beadle et al., 2008; Louis, 2006). Another advantage is the reduced number of cells required when compared to commonly used transwell migration assays. Furthermore, transwell assays fail to yield the information on migration and morphology of individual cells and only originate endpoint

information (Kim et al., 2009a). We found a substantial degree of heterogeneity in the glioblastoma samples analyzed. The increased average migration speed of a cell population in the presence of PDGF was ascribed to a small subpopulation of aggressive cells (approximately 25%). Knowledge of the degree of population heterogeneity can be critical to the decision-making in the clinic (Snuderl et al., 2011; Szerlip et al., 2012). In addition, our tissue mimetic platform can distinguish the effects of cell proliferation and migration phenotypes, which can be a confounding factor in both transwell and in vivo migration studies.

Our results also highlight advantages of the proposed method over traditional protein expression assays. We observed an incomplete correlation between receptor expression and response to PDGF signaling, possibly due to veiled differences in the signal transduction pathways. We demonstrated that protein expression analysis was less sensitive and less robust at predicting differences among patient tumor features. Genomic and proteomic approaches also suffer from limited supplies of primary tissues available for their cumbersome requirements of cellular material.

Overall, the results here support the proposed methodology as a simpler, more biomimetic, and informative method to gain critical information about patient tumors and cell populations. The analysis presented here reveals the importance of careful engineering of chemical and mechanical extracellular milieu in cell migration analysis. We believe that this methodology will provide an important prognostic tool, with benefits that include high-throughput, label-free analysis of single-cell resolution; low demand for precious primary cell samples; and better physiological relevance compared to other migration assays.

EXPERIMENTAL PROCEDURES

Cells

Human tissues were obtained at Johns Hopkins medical institutions and used with approval of the Institutional Review Board. Glioblastoma pathologically confirmed tumor samples (GBM 221, GBM 253, GBM 276, GBM 318, GBM 499, GBM 501, GBM 544, GBM 549, GBM 567, GBM 609, GBM 612, GBM 626, GBM 630, and GBM 854) were derived from primary intraoperative tissues of patients undergoing surgery. Tissue donors received no treatment before surgery.

Construction of a Multi-well Nanopatterned Device

The topographic nanopatterned substratum, consisting of parallel ridges 350 nm wide and 500 nm high that are spaced 1.5 μm apart, was fabricated onto glass coverslips as previously described (Kim et al., 2009a, 2009b) using UV-assisted capillary molding techniques.

Time-Lapse Microscopy of Live Cells and Quantitative Analysis of Cell Morphology and Migration

Cell migration was observed using time-lapse microscopy (Movies S1, S2, and S3). To enable long-term observation, the multi-well, nanopatterned device was mounted on the stage of a motorized inverted microscope (Olympus IX81) equipped with a Photometrics hCascade 512B II charge-coupled device camera and temperature- and gas-controlling environmental chamber. Phase-contrast cell images were automatically recorded under a 10 \times objective (numerical aperture = 0.30) using SlideBook 4.1 software (Intelligent Imaging Innovations) for 10–15 hr at 10 or 20 min intervals. Because cell-cell contact is known to affect the extent of cell spreading and migration, cells were plated at low density ($\sim 4 \times 10^4$ cells ml^{-1}) to allow isolated movements. A custom-made MATLAB script was used to allow manual tracking and measurement of cells frame by frame.

Tumor Xenografts

Animal protocols were approved by the Johns Hopkins School of Medicine Animal Care and Use Committee. For intracranial xenografts, severe combined immunodeficiency mice received 100,000 viable cells in 1 μl of DMEM/F12 serum media without growth factors by stereotactic injection into the right striatum. Cells were cultured in DMEM/F12 serum media with epidermal growth factor, fibroblast growth factor, and PDGF ligand for 3 weeks before injections were performed. Cell viability was determined by trypan blue dye exclusion. Mice were perfused with 4% paraformaldehyde at the indicated times, and the brains were removed for histological analysis.

Statistical Analysis

Results are presented as mean + SEM. The Mann-Whitney rank-sum test was for pairwise comparisons; Dunn's test (rank-based ANOVA) was used in multiple group comparisons. When noted, Student's *t* test or standard ANOVA (the Holm-Sidak method) was used. Univariate Cox analysis was used to identify correlations among tumor characteristics. To group data, thresholds were determined using linear discriminant analysis as previously described (Lin et al., 2012). Statistics were analyzed using Sigmaplot, GraphPad Prism, and MATLAB software.

SUPPLEMENTAL INFORMATION

Supplemental Information includes Supplemental Experimental Procedures, four figures, one table, and three movies and can be found with this article online at <http://dx.doi.org/10.1016/j.celrep.2016.05.042>.

AUTHOR CONTRIBUTIONS

Conceptualization, C.L.S., O.K., P.S., A.Q.-H., and A.L.; Analysis, C.L.S., O.K., P.S., F.J.R., and K.L.C.; Investigation, C.L.S., O.K., P.S., N.I.S.-R., H.G.-C., S.G., T.O., S.A., and J.P.; Writing, C.L.S., O.K., P.S., H.G.-C., A.Q.-H., and A.L.; Supervision, A.Q.-H. and A.L.

CONFLICTS OF INTEREST

Some authors are listed as inventors in pending patents (C.L.S., D.-H.K., O.K., P.S., A.Q.-H., and A.L.).

ACKNOWLEDGMENTS

We thank H. Basdag, L. Johnson, and L. Noiman for establishing cell cultures; H. Nam Kim and K.Y. Suh for help in building nanopatterned surfaces; and M. Delannoy for assistance with SEM. This work was funded by NIH R01 NS070024 (to A.Q.-H.), a Ford Foundation fellowship (to C.L.S.), AHA fellowship 13POST17140090 (to O.K.), and NIH grants U01CA15578 and CA16359 (Yale Cancer Center) (to A.L.).

Received: December 9, 2015

Revised: February 24, 2016

Accepted: May 9, 2016

Published: June 9, 2016

REFERENCES

- Anton, E.S., Kreidberg, J.A., and Rakic, P. (1999). Distinct functions of $\alpha 3$ and αv integrin receptors in neuronal migration and laminar organization of the cerebral cortex. *Neuron* 22, 277–289.
- Beadle, C., Assanah, M.C., Monzo, P., Vallee, R., Rosenfeld, S.S., and Canoll, P. (2008). The role of myosin II in glioma invasion of the brain. *Mol. Biol. Cell* 19, 3357–3368.
- Bellail, A.C., Hunter, S.B., Brat, D.J., Tan, C., and Van Meir, E.G. (2004). Micro-regional extracellular matrix heterogeneity in brain modulates glioma cell invasion. *Int. J. Biochem. Cell Biol.* 36, 1046–1069.

- Chaichana, K.L., Zadnik, P., Weingart, J.D., Olivi, A., Gallia, G.L., Blakeley, J., Lim, M., Brem, H., and Quiñones-Hinojosa, A. (2013). Multiple resections for patients with glioblastoma: prolonging survival. *J. Neurosurg.* *118*, 812–820.
- Chaichana, K.L., Jusue-Torres, I., Navarro-Ramirez, R., Raza, S.M., Pascual-Gallego, M., Ibrahim, A., Hernandez-Hermann, M., Gomez, L., Ye, X., Weingart, J.D., et al. (2014). Establishing percent resection and residual volume thresholds affecting survival and recurrence for patients with newly diagnosed intracranial glioblastoma. *Neuro Oncol.* *16*, 113–122.
- Doyle, A.D., Wang, F.W., Matsumoto, K., and Yamada, K.M. (2009). One-dimensional topography underlies three-dimensional fibrillar cell migration. *J. Cell Biol.* *184*, 481–490.
- Feng, H., Liu, K.W., Guo, P., Zhang, P., Cheng, T., McNiven, M.A., Johnson, G.R., Hu, B., and Cheng, S.Y. (2012). Dynamin 2 mediates PDGFR α -SHP-2-promoted glioblastoma growth and invasion. *Oncogene* *31*, 2691–2702.
- Filippini, G., Falcone, C., Boiardi, A., Broggi, G., Bruzzone, M.G., Caldiroli, D., Farina, R., Farinotti, M., Fariselli, L., Finocchiaro, G., et al.; Brain Cancer Register of the Fondazione IRCCS (Istituto Ricovero e Cura a Carattere Scientifico) Istituto Neurologico Carlo Besta (2008). Prognostic factors for survival in 676 consecutive patients with newly diagnosed primary glioblastoma. *Neuro-oncol.* *10*, 79–87.
- Fomchenko, E.I., and Holland, E.C. (2007). Platelet-derived growth factor-mediated gliomagenesis and brain tumor recruitment. *Neurosurg. Clin. N. Am.* *18*, 39–58, viii.
- Friedl, P., and Wolf, K. (2010). Plasticity of cell migration: a multiscale tuning model. *J. Cell Biol.* *188*, 11–19.
- Friedlander, D.R., Zagzag, D., Shiff, B., Cohen, H., Allen, J.C., Kelly, P.J., and Grumet, M. (1996). Migration of brain tumor cells on extracellular matrix proteins in vitro correlates with tumor type and grade and involves α V and β 1 integrins. *Cancer Res.* *56*, 1939–1947.
- Garzon-Muvdi, T., Schiapparelli, P., ap Rhys, C., Guerrero-Cazares, H., Smith, C., Kim, D.-H., Kone, L., Farber, H., Lee, D.Y., An, S.S., et al. (2012). Regulation of brain tumor dispersal by NKCC1 through a novel role in focal adhesion regulation. *PLoS Biol.* *10*, e1001320.
- Gonzalez-Perez, O., Guerrero-Cazares, H., and Quiñones-Hinojosa, A. (2010). Targeting of deep brain structures with microinjections for delivery of drugs, viral vectors, or cell transplants. *J. Vis. Exp.* (46), 2082.
- Goswami, C.P., and Nakshatri, H. (2013). PROGene: gene expression based survival analysis web application for multiple cancers. *J. Clin. Bioinforma.* *3*, 22.
- Huang, Y.-J., Hoffmann, G., Wheeler, B., Schiapparelli, P., Quinones-Hinojosa, A., and Searson, P. (2016). Cellular microenvironment modulates the galvanotaxis of brain tumor initiating cells. *Sci. Rep.* *6*, 21583.
- Jackson, E.L., Garcia-Verdugo, J.M., Gil-Perotin, S., Roy, M., Quinones-Hinojosa, A., VandenBerg, S., and Alvarez-Buylla, A. (2006). PDGFR α -positive B cells are neural stem cells in the adult SVZ that form glioma-like growths in response to increased PDGF signaling. *Neuron* *51*, 187–199.
- Kalisky, T., Blainey, P., and Quake, S.R. (2011). Genomic analysis at the single-cell level. *Annu. Rev. Genet.* *45*, 431–445.
- Kim, D.-H., Han, K., Gupta, K., Kwon, K.W., Suh, K.-Y., and Levchenko, A. (2009a). Mechanosensitivity of fibroblast cell shape and movement to anisotropic substratum topography gradients. *Biomaterials* *30*, 5433–5444.
- Kim, D.-H., Seo, C.-H., Han, K., Kwon, K.W., Levchenko, A., and Suh, K.-Y. (2009b). Guided cell migration on microtextured substrates with variable local density and anisotropy. *Adv. Funct. Mater.* *19*, 1579–1586.
- Kim, D.H., Provenzano, P.P., Smith, C.L., and Levchenko, A. (2012). Matrix nanotopography as a regulator of cell function. *J. Cell Biol.* *197*, 351–360.
- Laurent, M., Martinerie, C., Thibout, H., Hoffman, M.P., Verrecchia, F., Le Bouc, Y., Mauviel, A., and Kleinman, H.K. (2003). NOVH increases MMP3 expression and cell migration in glioblastoma cells via a PDGFR- α -dependent mechanism. *FASEB J.* *17*, 1919–1921.
- Lin, B., Holmes, W.R., Wang, C.J., Ueno, T., Harwell, A., Edelstein-Keshet, L., Inoue, T., and Levchenko, A. (2012). Synthetic spatially graded Rac activation drives cell polarization and movement. *Proc. Natl. Acad. Sci. USA* *109*, E3668–E3677.
- Lokker, N.A., Sullivan, C.M., Hollenbach, S.J., Israel, M.A., and Giese, N.A. (2002). Platelet-derived growth factor (PDGF) autocrine signaling regulates survival and mitogenic pathways in glioblastoma cells: evidence that the novel PDGF-C and PDGF-D ligands may play a role in the development of brain tumors. *Cancer Res.* *62*, 3729–3735.
- Louis, D.N. (2006). Molecular pathology of malignant gliomas. *Annu. Rev. Pathol.* *1*, 97–117.
- McGirt, M.J., Chaichana, K.L., Gathinji, M., Attenello, F.J., Than, K., Olivi, A., Weingart, J.D., Brem, H., and Quiñones-Hinojosa, A.R. (2009). Independent association of extent of resection with survival in patients with malignant brain astrocytoma. *J. Neurosurg.* *110*, 156–162.
- Meier, M., Sit, R.V., and Quake, S.R. (2013). Proteome-wide protein interaction measurements of bacterial proteins of unknown function. *Proc. Natl. Acad. Sci. USA* *110*, 477–482.
- Ottani, V., Raspanti, M., and Ruggeri, A. (2001). Collagen structure and functional implications. *Micron* *32*, 251–260.
- Park, J., Kim, D.H., Kim, H.N., Wang, C.J., Kwak, M.K., Hur, E., Suh, K.Y., An, S.S., and Levchenko, A. (2016). Directed migration of cancer cells guided by the graded texture of the underlying matrix. *Nat. Mater.* Published online March 14, 2016. <http://dx.doi.org/10.1038/nmat4586>.
- Petrie, R.J., Doyle, A.D., and Yamada, K.M. (2009). Random versus directionally persistent cell migration. *Nat. Rev. Mol. Cell Biol.* *10*, 538–549.
- Porcionatto, M.A. (2006). The extracellular matrix provides directional cues for neuronal migration during cerebellar development. *Braz. J. Med. Biol. Res.* *39*, 313–320.
- Sahai, E. (2007). Illuminating the metastatic process. *Nat. Rev. Cancer* *7*, 737–749.
- Shih, A.H., and Holland, E.C. (2006). Platelet-derived growth factor (PDGF) and glial tumorigenesis. *Cancer Lett.* *232*, 139–147.
- Snuderl, M., Fazlollahi, L., Le, L.P., Nitta, M., Zhelyazkova, B.H., Davidson, C.J., Akhavanfard, S., Cahill, D.P., Aldape, K.D., Betensky, R.A., et al. (2011). Mosaic amplification of multiple receptor tyrosine kinase genes in glioblastoma. *Cancer Cell* *20*, 810–817.
- Szerlip, N.J., Pedraza, A., Chakravarty, D., Azim, M., McGuire, J., Fang, Y., Ozawa, T., Holland, E.C., Huse, J.T., Jhanwar, S., et al. (2012). Intratumoral heterogeneity of receptor tyrosine kinases EGFR and PDGFRA amplification in glioblastoma defines subpopulations with distinct growth factor response. *Proc. Natl. Acad. Sci. USA* *109*, 3041–3046.
- Verhaak, R.G.W., Hoadley, K.A., Purdom, E., Wang, V., Qi, Y., Wilkerson, M.D., Miller, C.R., Ding, L., Golub, T., Mesirov, J.P., et al.; Cancer Genome Atlas Research Network (2010). Integrated genomic analysis identifies clinically relevant subtypes of glioblastoma characterized by abnormalities in PDGFRA, IDH1, EGFR, and NF1. *Cancer Cell* *17*, 98–110.
- Wirtz, D., Konstantopoulos, K., and Searson, P.C. (2011). The physics of cancer: the role of physical interactions and mechanical forces in metastasis. *Nat. Rev. Cancer* *11*, 512–522.